

DNA polymerase activities of these clones were assayed. We observed no significant variation in the specific activity of DNA polymerase (nanomoles of dTMP per milligram of protein, 20 minutes at 37°C) in mitochondria-free crude extracts from wild-type (2.7), Aph^r-4-2 (1.7), and AphVT-1 (2.4) cells. Figure 1B shows that wild-type DNA Pol- α was sensitive to $>0.2 \mu\text{M}$ aphidicolin. In three separate experiments, the DNA Pol- α activity (mean \pm standard error) was decreased by 59 ± 4 percent for wild-type, 13 ± 11 percent for Aph^r-4-2, and 23 ± 5 percent for AphVT-1 by the presence of $0.6 \mu\text{M}$ aphidicolin (data not shown). Thus the mutant Pol- α is stably expressed in the transfectant.

In cotransfer experiments with the thymidine kinase (*tk*) gene and the β -globin gene into murine thymidine kinase-deficient Ltk⁻ cells with single selection for *tk*⁺ transfectants, Wigler *et al.* (12) and Huttner *et al.* (13) found that more than 75 percent of the *tk*⁺ transfectants contained the integrated β -globin gene. Similarly, after cotransfection of pSV2-gpt and HeLa DNA into mitomycin-C-sensitive Chinese hamster ovary (CHO) cells, and selection for both MAX^r and mitomycin-C-resistant transfectants, Rubin *et al.* (14) have found that 2 of the 800 MAX^r clones (≤ 0.3 percent) contained human sequences and were mitomycin-C-resistant. With selections for both markers, we found that 20 percent of MAX^r clones were MAX^rAph^r. Because the background frequency was less than 10^{-6} for MAX^r and less than 10^{-7} for Aph^r colonies, the chance to obtain a colony that spontaneously exhibited both MAX^r and Aph^r phenotypes would be less than 10^{-13} . The transfection efficiency of 4 per 10^7 per microgram of mutant DNA is 10^6 times higher than that expected from two independent spontaneous mutations. Taken together, our data indicate that the Aph^r colonies are the result of DNA-mediated gene transfer; a DNA fragment presumably greater than 5 kb, rendering cells aphidicolin resistant, had been transferred via DNA-mediated transfection of V79 wild-type cells. Our studies suggest that Aph^r phenotype can be used as a selectable marker for the transfection of the gene for DNA Pol- α , further providing evidence that Aph^r-4-2 is a mutant with a defect in the gene for DNA Pol- α .

PHILIP K. LIU
LAWRENCE A. LOEB

Joseph Gottstein Memorial Cancer
Research Laboratory, Department of
Pathology, University of Washington,
Seattle 98195

16 NOVEMBER 1984

References and Notes

1. A. Kornberg, *DNA Replication* (Freeman, San Francisco, 1980).
2. C.-c. Chang *et al.*, *Somat. Cell Genet.* 7, 235 (1981).
3. P. K. Liu, C.-c. Chang, J. E. Trosko, D. K. Dube, G. M. Martin, L. A. Loeb, *Proc. Natl. Acad. Sci. U.S.A.* 80, 797 (1983).
4. P. K. Liu, C.-c. Chang, J. E. Trosko, *Mutat. Res.* 106, 317 (1982); P. K. Liu, J. E. Trosko, C.-c. Chang, *ibid.*, p. 333; P. K. Liu, C.-c. Chang, J. E. Trosko, *Somat. Cell Mol. Genet.* 10, 235 (1984).
5. F. J. Bollum, *Prog. Nucleic Acid Res. Mol. Biol.* 15, 109 (1975); P. A. Fisher and D. Korn, *J. Biol. Chem.* 252, 6528 (1977); E. Karawya and S. H. Wilson, *ibid.* 257, 13129 (1982); D. K. Dube, E. C. Travaglini, L. A. Loeb, in *Methods in Cell Biology*, D. M. Prescott, Ed. (Interprint LTD, Malta, 1978), pp. 27-42; D. Filipula, P. A. Fisher, D. Korn, *J. Biol. Chem.* 257, 2029 (1982).
6. S. Ikegami, T. Taguchi, M. Ohashi, M. Oguro, H. Nagano, Y. Mano, *Nature (London)* 275, 458 (1978); J. A. Huberman, *Cell* 23, 647 (1981).
7. M. Oguro, M. Shioda, H. Nagano, Y. Mano, F. Hanoaka, Y. Yamada, *Biochem. Biophys. Res. Commun.* 92, 13 (1980); A. M. Holmes, *Nucleic Acids Res.* 9, 161 (1981).
8. C.-c. Chang, P. K. Liu, J. E. Trosko, Abstract Fb-5, Fifteenth Annual meeting, Environmental Mutagen Society, Montreal, Quebec, Canada, February 1984.
9. C. D. Whitfield, R. Bostedor, D. Goodrum, M. Haak, E. H. Y. Chu, *J. Biol. Chem.* 256, 6651 (1981).
10. M. Wigler, A. Pellicer, S. Silverstein, R. Axel, G. Urlaub, L. Chasin, *Proc. Natl. Acad. Sci. U.S.A.* 76, 1373 (1979); C. M. Corsaro and M. L. Pearson *Somat. Cell Genet.* 7, 603 (1981).
11. R. C. Mulligan and P. Berg, *Proc. Natl. Acad. Sci. U.S.A.* 78, 2072 (1981). MAX is mycophenolic acid (20 $\mu\text{g/ml}$), adenine (25 $\mu\text{g/ml}$), and xanthine (200 $\mu\text{g/ml}$).
12. M. Wigler *et al.*, *Cell* 16, 777 (1979).
13. K. M. Huttner, G. Scangos, F. H. Ruddle, *Proc. Natl. Acad. Sci. U.S.A.* 76, 5820 (1979); G. Scangos and F. H. Ruddle, *Gene* 14, 1 (1981).
14. J. S. Rubin, A. L. Joyner, A. Bernstein, G. F. Whitmore, *Nature (London)* 306, 206 (1983).
15. T. Maniatis, E. F. Fritsch, J. Sambrook, in *Molecular Cloning: A Laboratory Manual* (Cold Spring Harbor Laboratory, Cold Spring Harbor, N.Y., 1982), p. 86.
16. D. Ayusawa, K. Iwata, T. Seno, *Somat. Cell Genet.* 7, 27 (1980); C. L. K. Sabourin, P. F. Bates, L. Glatzer, C.-c. Chang, J. E. Trosko, J. A. Boezi, *ibid.*, p. 255.
17. R. R. Sokal and F. J. Rohlf, *Biometry, The Principles and Practice of Statistics in Biological Research* (Freeman, San Francisco, 1969).
18. We thank C. Shearman, S. Garter, T. Norwood, R. Monnat, C.-c. Chang, and D. Dube for generous counsel, B. Douros of the National Cancer Institute for aphidicolin, M. Wade of Michigan State University for pSV2-gpt, R. Palmer of the University of Washington for standard pSV2-gpt, S. Fredell for technical assistance, and J. Hiltner for word processing. This investigation was supported by grants from NIH (CA24845) and DOE (DE-AT06-82ER60069) to L.A.L. P.K.L. is a postdoctoral fellow of the National Cancer Institute (CA07418).

22 March 1984; accepted 3 August 1984

Ion Channels in Plasmalemma of Wheat Protoplasts

Abstract. *The patch-clamp technique was used to study passive movements of ions through the plasmalemma of wheat leaf protoplasts. This method overcomes the problems inherent in conventional electrophysiological study of plant cells. Changes in conductance were recorded in patches excised from the plasmalemma. Two types of patches were observed: (i) regions of low channel density, where discrete single-channel currents could be resolved and conductance ranged from 10 to 200 picosiemens and (ii) regions of high channel density, where single-channel currents could not be resolved and conductance was on the order of a few nanosiemens. The results indicate a striking similarity between animal and plant cell membranes in the basic phenomena of transport. Moreover, the approach used constitutes a new degree of refinement in the study of processes of regulation, pathology, and toxicity in plants.*

While electrogenic ion pumps, along with other carrier mechanisms, have an important role in plant ion transport (1), relatively little is known about the passive ion pathways, in particular about gated channels, such as those observed in animal cells (2). One reason for this is the difficulty in using electrophysiological methods to study ion movements in plant cells (1). This difficulty stems largely from the specific compartmentalization of the cell. Most of the volume of plant cells is occupied by a vacuole, with a very thin layer of organelle-packed cytoplasm separating the outer membrane (the plasmalemma) from the membrane of the vacuole (the tonoplast). It is, therefore, not a simple task to locate the tip of an inserted microelectrode with respect to the membranes. Until recently, successful attempts at voltage clamping plant cells required the use of large cells from algae, such as *Nitella* (3),

Chara (4, 5), and *Hydrodictyon* (6). In higher plants electrophysiology has, to our knowledge, been limited to measurements of membrane resistance and membrane potential (7-13). Accurate measurements of potentials across the plasmalemma are impeded by the cell wall in series with the plasmalemma. Because of its fixed negative charges, the cell wall adds an unknown voltage component to the measurement.

In this study we examined separately the pathways of passive ion movement in an attempt to distinguish between carrier and gated-channel modes of transport. To overcome the difficulties described above we combined the technique of enzymatic isolation of plant protoplasts devoid of cell walls with the voltage-clamp technique by using a "patch electrode."

Leaf protoplasts were isolated from 7-day-old wheat plants (*Triticum aestivum*)

(14). The protoplasts were purified on a sucrose gradient and transferred to a 35-mm tissue culture dish (Primaria, Falcon). The experiments were performed at 22° to 24°C. Our recording medium consisted of 0.4M mannitol or sorbitol, 50 mM NaCl, 1 mM CaCl₂ (or up to 10 mM, where indicated) and was buffered with 5 to 10 mM Hepes or 2-(N-morpholino)ethane sulfonic acid to pH 5.8 to 6.2. In some cases NaCl was substituted with 50 mM sodium gluconate, KCl, or 25 mM LaCl₃. A patch-clamp system (List

Electronics) was used to voltage clamp the membrane in an excised-patch configuration (15). The output current from the membrane patch was filtered through a four-pole Butterworth filter (Krohn-Hite) at 2.5-kHz low-pass resistance-capacitance mode and digitized at 10 kHz. The patch electrode was fabricated from soft (soda-lime) glass by the method of Hamill *et al.* (15) and coated with wax. The tip diameter of the electrode was <1 μm and its resistance was 7 to 12 megohms. The solution in the patch pi-

pette was similar to the external solution, unless otherwise indicated. Potential was measured with Ag-AgCl electrodes (E. W. Wright).

The prerequisite for recording a single-channel current is the establishment of a "gigohm seal" (10 to 50 gigohms) between the electrode and the cell membrane. In our preparation the cell membrane was fragile, breaking on very gentle suction (as marked by an increase of the capacitive transient of current in response to a test pulse), usually before a gigohm seal was established. The resistance measured at the electrode would then increase spontaneously to a few hundred megohms. This was probably caused by the establishment of a seal between the rim of the pipette and the plasmalemma. Tonoplast involvement was unlikely, since a soft glass electrode is not expected to form a gigohm seal with another membrane (the tonoplast) after touching the plasmalemma. At this stage a whole-cell voltage clamp could be obtained. The internal milieu of the cytoplasm was rapidly exchanged with that of the pipette (in a matter of seconds in the case of a 30- to 40-μm cell). On withdrawal of the pipette the resistance would increase further to several gigohms, in which case we assumed, in accordance with accepted practice (15), to have obtained an excised "outside-out" patch. Our success rate at obtaining a gigohm seal on withdrawal was 5 to 10 percent of attempted cell-pipette contacts. Considerably fewer successful patches were achieved in the "inside-out" configuration, formed by pulling away without breaking into the cell first.

In 23 of 41 excised patches, discrete current fluctuations were observed at constant membrane potential (Fig. 1A). The fluctuations represent the opening and closing of individual ion channels. Figure 1B depicts the current-voltage relation of the single channel represented in Fig. 1A. The slope of the relation is constant over the examined voltage range, yielding a conductance, in this case, of ~35 pS. Conductance is used as one characteristic of channels. We grouped channels into four classes according to their conductance: 10 to 20 pS (Fig. 2, A and B), 35 to 40 pS (Fig. 1), 70 to 100 pS (Fig. 2C), and 160 to 180 pS (Fig. 2D).

A patch sometimes contained only one channel; more frequently, it contained two or three types of channels. Sometimes seven or ten channels of the same type (as judged by amplitude and voltage dependence) appeared simultaneously (Fig. 1A). We did not observe, however,

Fig. 1. Voltage-dependent single-channel currents in an inside-out patch bathed in NaCl medium on both sides (10 mM CaCl₂ was added to the pipette). (A) Current fluctuations at different membrane depolarizing potentials, indicated to the right. Downward deflection indicates channel opening. Note the multilevel jumps, indicating the presence of several channels in the patch (the existence of seven was assumed for the calculations). (B) Current-voltage relation for a single open channel. The conductance of this channel was 35 pS. (C) Open probability versus membrane potential, estimated by fitting amplitude histograms of the records with the calculated binomial distribution of relative fraction of time spent in each of the different levels.

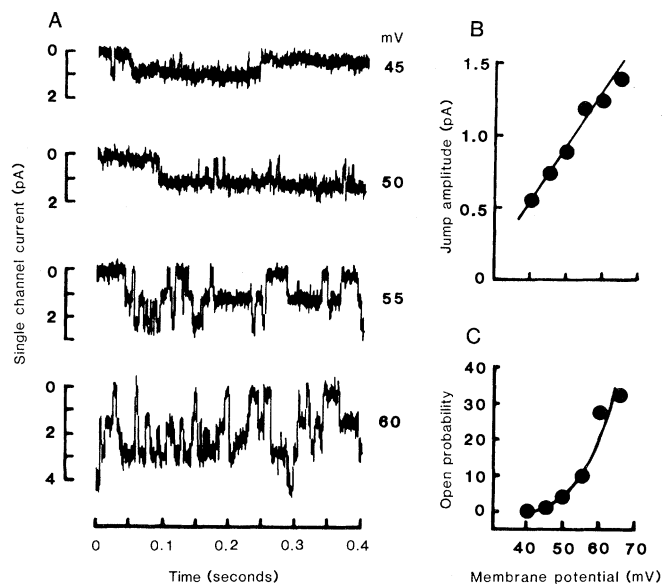
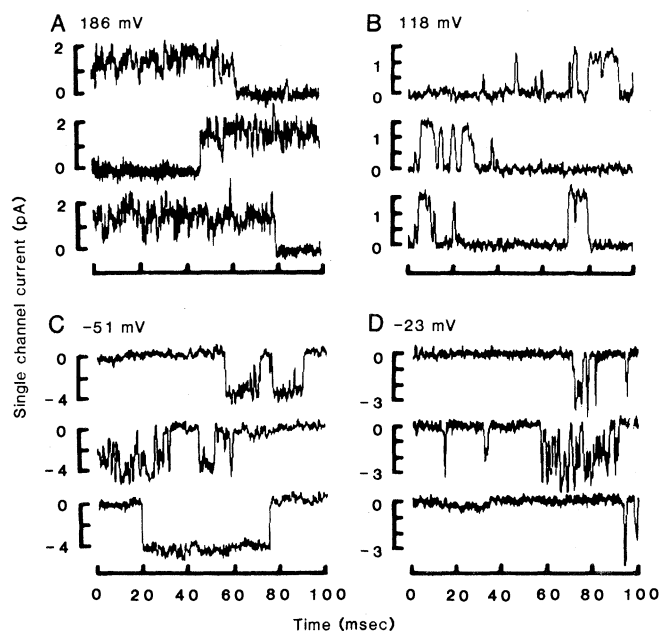


Fig. 2. Various types of single-channel currents in four excised, outside-out, low-density patches. Sample records are at indicated membrane potentials. Positive values denote depolarization and outward current; negative values, hyperpolarization and inward current (0 marks the level of current when the channel is closed). Channel conductances are (A) 8 pS (membrane was bathed in 50 mM NaCl with 10 mM CaCl₂ added outside), (B) 16 pS (medium contained 50 mM NaCl), (C) 80 pS (50 mM sodium gluconate), and (D) 160 pS (50 mM sodium gluconate).



more than two channels of the large type (70 to 180 pS) in a single patch.

So far, our information concerning the selectivity of the channels is scant. The currents depicted in Fig. 2, C and D, are probably carried by cations (Na^+), since the prevalent anion in the recording medium was gluconate, a nonpermeant species.

The observed kinetic behavior of the channels varied considerably. Some of the openings appeared to be evenly distributed in time (Fig. 2B), with mean open time ranging from 1 to 100 msec, while others occurred in bursts of rapid flickering (rapid transitions between closed and open states) (Fig. 2, A and D). Bursts lasted tens (Fig. 2D) to hundreds (Fig. 2A) of milliseconds.

In five cases of the single-channel recordings, the probability of opening was strongly dependent on membrane potential (Fig. 1, A and C). The voltage-dependent channels belonged mainly to the 40-pS class of channels. They opened randomly for a few milliseconds to a few tens of milliseconds. Voltage dependence of gating is characteristic of many types of channels in animal cells—for example, sodium channels in neurons or muscle cells.

In about 40 percent of all cases, the response of an excised patch to square voltage pulses was a current that varied smoothly with time (Fig. 3A), with relaxation times ranging from 100 msec to a few seconds. We refer to these currents as macroscopic. Figure 3B summarizes their asymmetrical current-voltage relation. The smooth appearance of the macroscopic currents (Fig. 3A) may indicate that many small channels contribute to the record. From the small noise-to-signal ratio of the currents (<5 percent), we estimate the number of channels to be more than 400 (16). This in turn places an upper bound on the single-channel conductance at 5 pS. The existence, in the small area of a patch (1 to 10 μm^2), of hundreds of channels ("hot spots") has been a common finding in animal cells, as in neuromuscular junctions (17).

The macroscopic currents for these high-density patches showed voltage dependence (Fig. 3A). The single-channel events from the low-density patches were much more steeply voltage-dependent than the macroscopic currents. We have not yet recorded isolated single-channel events directly corresponding to these macroscopic currents. It is possible, therefore, that the channels underlying the macroscopic currents exist predominantly in hot spots. Conversely, the single voltage-dependent channels might

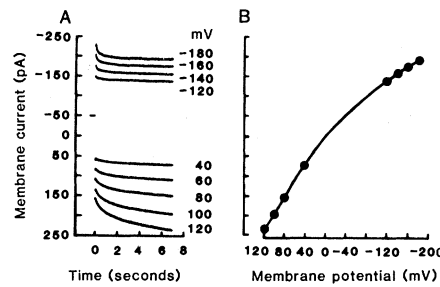


Fig. 3. Macroscopic currents in an excised, high-density patch elicited by voltage-clamp pulses starting at time 0. Values of potential are indicated to the right of the current traces. Positive numbers indicate depolarizing potentials and outward currents; negative numbers, hyperpolarization and inward currents. An outside-out patch, held at -40 mV between pulses, is represented. (A) Time course of the currents. (B) Current-voltage relation for currents shown in (A), at the end of 5-second pulses. Conductance is asymmetrical with respect to voltage: 2 nS at depolarization and 0.9 nS at hyperpolarization. The membrane was bathed in 25 mM LaCl_3 medium on both sides. Since La^{3+} has been shown to block channels (20) rather than to permeate them, it is likely that these currents are carried by Cl^- .

not form hot spots. Similar variability in spatial distribution has been observed between the sodium channels (forming aggregates) and potassium channels (more evenly distributed) in muscle (18).

For both the voltage-dependent channels from the low-density patches and for the channels underlying the currents from the high-density patches, the probability of being open usually increased with depolarization. However, in about 10 percent of the cases the probability increased on hyperpolarization. In spite of the possible ambiguity concerning patch polarity, we believe that our findings reflect the real situation—that in some cases, hyperpolarization rather than depolarization opens the channel, as occurs with the anomalous rectifier (19). Moreover, Findlay *et al.* (6) recorded a similar finding in voltage-clamped *Hydrodictyon*.

Voltage clamping of an excised patch offers the advantage of examining the passive ion transport separately from that mediated by the electrogenic pump. In our experiments we can eliminate the latter, since the patches of the two types (both the low- and the high-density ones) were bathed in controlled (usually symmetrical) solutions on both sides, without adenosine triphosphate or any other source of energy to drive the electrogenic pump. Any significant concentration of such compound of cellular origin near the membrane would have dissipated within seconds, while our experiments

usually lasted from 30 minutes to 3 hours.

At present we are unable to eliminate the possibility that the macroscopic currents are, at least in some cases, the response of passive ion carriers rather than channels, except that it seems difficult to explain the asymmetry of carrier-mediated current with respect to voltage in symmetrical solutions.

In contrast to macroscopic currents from high-density patches, current fluctuations from low-density patches unequivocally show the existence of gated channels in plant plasmalemma. From the single-channel measurements we calculate the rate of ion transfer through a 20-pS channel, at a membrane potential of 100 mV, to be about 10^7 ions per second. This is about 1000 times faster than the turnover rate of one of the fastest carriers known, valinomycin. In addition, it is hard to envision a process that would synchronize thousands of carrier molecules (were they all concentrated in the patch area to produce the recorded discrete fluctuations of current).

While we do not know what fraction of ion transport occurs through channels, the variety of channel types reported here suggests a multitude of functions involving ion movement through the membranes of higher plants.

NAVA MORAN
GERALD EHRENSTEIN
KUNIHICO IWASA

Laboratory of Biophysics, National
Institute of Neurological and
Communicative Disorders and Stroke,
Bethesda, Maryland 20205

CHARLES BARE, CHARLES MISCHKE
Agricultural Research Service,
Weed Science Laboratory, Agricultural
Environmental Quality Institute,
Beltsville, Maryland 20705

References and Notes

1. R. M. Spanswick, *Annu. Rev. Plant Physiol.* **32**, 267 (1981).
2. D. T. Clarkson, *Advanced Plant Physiology* (Pitman, Marshfield, Mass., 1984), pp. 319-353.
3. U. Kishimoto, *J. Cell. Comp. Physiol.* **66**, 43 (1965).
4. M. J. Bielby and H. G. L. Coster, *Aust. J. Plant Physiol.* **6**, 323 (1979).
5. P. T. Smith and N. A. Walker, *J. Membr. Biol.* **60**, 273 (1981).
6. G. P. Findlay and H. A. Coleman, *ibid.* **75**, 241 (1983).
7. B. Etherton and N. Higinbotham, *Science* **131**, 409 (1960).
8. R. M. Spanswick, *Planta* **102**, 215 (1972).
9. D. P. Briskin and R. T. Leonard, *Plant Physiol.* **64**, 959 (1979).
10. R. L. Satter and A. W. Galston, *Annu. Rev. Plant Physiol.* **32**, 83 (1981).
11. C. D. Kennedy and R. A. Stuart, *J. Exp. Bot.* **33**, 1220 (1982).
12. N. Siegel and A. Huag, *Physiol. Plant.* **59**, 285 (1983).
13. K. Schefczik, W. Simonis, M. Schiebe, *Plant Physiol.* **72**, 368 (1983).
14. G. E. Edwards, S. P. Robinson, N. J. C. Tyler, D. A. Walker, *ibid.* **62**, 313 (1978).

15. O. P. Hamill, A. Marty, E. Neher, B. Sackmann, F. J. Sigworth, *Pfluegers Arch.* **391**, 85 (1981).
16. H. Lecar and R. Nossal, *Biophys. J.* **11**, 1068 (1971).
17. V. Dionne and M. D. Leibovitz, *ibid.* **39**, 253 (1982).
18. W. Almers, P. R. Stanfield, W. Stuhmer, *J. Physiol. (London)* **336**, 261 (1983).
19. H. Ohmori, S. Yoshida, S. Hagiwara, *Proc. Natl. Acad. Sci. U.S.A.* **78**, 4960 (1981).
20. M. M. Boucek and R. Snyderman, *Science* **193**, 905 (1976).
21. We are grateful to H. Lecar for his helpful comments and to A. Chang for technical assistance.

2 July 1984; accepted 20 August 1984

A Major Human Histone Gene Cluster on the Long Arm of Chromosome 1

Abstract. A human histone gene cluster was assigned to chromosome 1 by Southern blot analysis of DNA's from a series of mouse-human somatic cell hybrids with ³²P-labeled cloned human H4 and H3 histone DNA as probes. Localization of this histone gene cluster on the long arm of chromosome 1 was confirmed by *in situ* hybridization of this DNA probe to metaphase chromosomes.

Human histone genes constitute a multigene family of moderately repeated sequences with variations in the structure, organization, and regulation of different copies (1-4). Yet our understanding of human histone gene organization is restricted to the observations that both core and H1 histone genes are clustered but not represented as simple tandem repeats (1, 2, 4) and that a limited number of histone sequences are nonfunctional pseudogenes (3). To further address the organization of human histone genes, we have focused on a histone gene cluster designated λHHG41 containing H4 and H3 histone coding sequences, the transcripts of which are predominant histone messenger RNA (mRNA) species associated with polyploids of cells undergoing DNA replication (5, 6).

Somatic cell hybrids with limited numbers of human chromosomes combined with probes for specific copies of the human histone genes provide a high resolution approach for chromosomal assignment of the various members of the histone gene family. DNA's from a series of mouse-human hybrid cells were digested with restriction endonucleases, fractionated electrophoretically, and, after transfer to nitrocellulose, were hybridized with ³²P-labeled (nick-translated) human H4 and H3 histone gene fragments subcloned from the λHHG41 genomic DNA cluster (Fig. 1A). The probes included flanking sequences to facilitate identification of these specific copies of the histone genes in Southern blots of total genomic DNA, and particularly, to distinguish between human and murine histone coding sequences.

Our initial studies, which were restricted to hybrid cells containing human chromosome 7, were based on reports that human histone genes are located on this chromosome (7, 8). Figure 1, B and C, clearly indicates that both the H4 and H3 histone genes that reside in the human DNA segment cloned in λHHG41 can be identified in restriction endonuclease-digested DNA from human cells and that a comparable gene is not observed in mouse cells. The absence of the H4 and H3 λHHG41 histone genes in the well-characterized hybrid cell line Nu9, which contains only human chromosomes 6 and 7 (9), was unexpected and provided the first indication that this gene cluster resides on another human chromosome (Fig. 1, B and C). The absence of this human histone gene cluster on chromosome 7 was substantiated by similar analysis of other human chromosome 7-containing hybrids. We then systematically analyzed Southern blots of genomic DNA's from an extensive series of mouse-human somatic cell hybrids that collectively contain all human chromosomes (9, 10). The hybrid cell lines used in these studies were derived from several different sets of human and mouse parentals, but gave consistent results establishing the location of the λHHG41 human histone gene cluster on chromosome 1 (Fig. 1D and Table 1). The H4 and H3 histone genes of λHHG41 have previously been mapped to 2.0- (H4) and 7.0-kilobase (H3) Hind III fragments of genomic DNA's from a number of human cells, including diploid, transformed, and tumor cell lines

Table 1. Representation of human histone genes in DNA's from a panel of mouse-human somatic cell hybrids representing the complete complement of human chromosomes. DNA (15 μg) from the designated hybrid cell lines were digested to completion with the restriction endonuclease Hind III, fractionated electrophoretically, and transferred to nitrocellulose. DNA's from human and mouse cell lines were included in all experiments as controls along with Hind III-digested λ phage as molecular weight markers. The DNA's immobilized on the filter were hybridized with ³²P-labeled human H4 or H3 histone genes representing the genomic DNA cluster λHHG41 and analyzed by autoradiography. Each DNA preparation was subjected to Southern blot analysis at least twice, and two or more DNA preparations from each hybrid cell line were analyzed. The construction and characterization of the various somatic cell hybrids have been reported (9, 10).

Hybrids	Chromosomes																						H3	H4	
	1	2	3	4	5	6	7	8	9	10	11	12	13	14	15	16	17	18	19	20	21	22			X
PT47C/3																		X				X	-	-	
1P1							X			X				X				X					X	-	-
Nu9						X	X																	-	-
CMC2859																					X			-	-
53-83-3C/10							X																	-	-
M44295														X										-	-
DSK13II2A5C/2			X					X						X		X	X					X		-	-
DSK13II2A5C/20														X	X	X	X	X			X	X		-	-
77B10C/30TK ⁺			X		X					X				X	X			X	X		X		X	-	-
77B10C/31TK ⁺	X		X		X			X	X	X				X	X			X	X		X		X	+	+
53-83-3C/21							X																	-	-
D2C16S3			X	X		X				X				X	X			X				X		-	-
CSK-N9-51C1-C/11	X			X				X		X	X	X	X	X	X	X	X	X	X	X	X	X	X	+	+
57-77-F7DC7					X								X	X	X								X	-	-
PAFBalbIVC/5		X			X			X					X	X	X					X				-	-
GM119XLMTK ⁻ C/3				X											X			X			X			-	-
GM119XLMTK ⁻ C/5				X				X				X			X						X		X	-	-